

## Direct Force Measurements between Dissimilar Metal Oxides<sup>†</sup>

Ian Larson,<sup>‡</sup> Calum J. Drummond,<sup>\*,§</sup> Derek Y. C. Chan,<sup>‡</sup> and Franz Grieser<sup>\*,‡</sup>

Advanced Mineral Products Special Research Centre, University of Melbourne, Parkville, 3052 Australia, and CSIRO Division of Chemicals and Polymers, Private Bag 10, Rosebank MDC, Clayton, 3169 Australia

Received: September 1, 1994; In Final Form: November 15, 1994<sup>⊗</sup>

An atomic force microscope has been used to measure the force of interaction between a SiO<sub>2</sub> glass sphere (~5 μm diameter) and a TiO<sub>2</sub> crystal, in an aqueous medium over the pH range 3–9. The force–separation profiles obtained were compared with DLVO theory, which was found to adequately account for the experimental results up to separations of ca. 2 nm. At distances below this point repulsive interactions in excess of DLVO may be present under certain conditions. To complement the diffuse layer potential results extracted from the force–separation data for dissimilar materials, force–separation interactions were also measured between two SiO<sub>2</sub> glass spheres. For both sets of surfaces, modeling of the experimental force–separation curves was best achieved using constant-charge rather than constant-potential boundary conditions.

### Introduction

The development of the atomic force microscope<sup>1</sup> (AFM) has made it possible to study directly the total force of interaction between a colloidal particle and, usually, a flat surface as a function of separation. AFM force measurements are normally made between a colloidal sphere glued to a cantilever spring and a flat surface which is driven toward and away from the cantilever with which the force is monitored. In the past 4 years the AFM has been used to measure a variety of forces in a liquid, usually aqueous, environment, including electrical double-layer forces (attractive and repulsive), van der Waals, as well as polymer depletion, steric, hydration, and hydrophobic interactions.<sup>2–5</sup> However, the majority of AFM work has involved the measurement of the double-layer repulsion between two similarly charged surfaces by collecting force versus separation curves over a range of pH and electrolyte conditions. By fitting these force–separation curves with solutions of the nonlinearized Poisson–Boltzmann equation according to DLVO theory,<sup>6</sup> it is possible to obtain the diffuse layer potential of the material being studied.

The calculation of electrical double layer interactions between dissimilarly charged surfaces acting under constant charge or constant potential boundary conditions can be quite complex. Consequently the theory of Hogg et al.<sup>7</sup> has been widely used in the past because of its relatively simple form, but this theory is strictly limited to low-potential systems, <25 mV, acting under constant-potential conditions. A new algorithm developed by McCormack et al.<sup>8</sup> for determining the electrical double-layer interaction between dissimilar surfaces has facilitated an accurate interpretation of force measurements between different materials in the AFM.

In this paper we report measurements of the forces of interaction between a spherical SiO<sub>2</sub> glass particle and a polished rutile titania single crystal. Silica and titania were chosen because of the vast information available on these materials and because we have already examined the rutile–rutile interaction in a previous study.<sup>3</sup> As the two materials have quite different isoelectric points (iep), this made it possible to measure the

interaction between two oppositely charged surfaces at pH values between the iep values of the two oxides.

For comparison we have also measured the total forces of interaction between two silica spheres with the AFM and calculated their diffuse layer potential from the silica–silica interaction. In addition, ζ potentials obtained from microelectrophoresis measurements on a sample of colloidal titania<sup>3</sup> are compared to the diffuse-layer potentials measured in the dissimilar system.

### Theory

In the case of interacting identically charged materials, the theory of Derjaguin–Landau–Verwey–Overbeek<sup>6</sup> (DLVO) separates the total interaction into two contributions: an attractive van der Waals interaction and an electrical double-layer repulsion. Importantly, the total interaction free energy can be taken as the sum of these two contributions. For dissimilar metal oxide surfaces interacting across water the van der Waals contribution will generally be attractive. However, if the interacting surfaces have dissimilar charges, the electrical double-layer contribution can be either attractive or repulsive or can even change from one to the other through charge regulation with changes in separation.<sup>7–9</sup>

When AFM measurements are made between two colloidal spheres, radii  $R_1$  and  $R_2$ , the Derjaguin approximation<sup>10</sup> relates the interaction free energy per unit area between parallel plates to the force ( $F$ ) between the spheres scaled by the effective radius  $R_T$ , where

$$\frac{1}{R_T} = \frac{1}{R_1} + \frac{1}{R_2}$$

(If the measurements are made between a sphere and a flat plate rather than between two spheres,  $R_2 \rightarrow \infty$ .) By

$$F/R_T = 2\pi(V_A + V_R)$$

Here  $V_A$  is the van der Waals interaction free energy per unit area and  $V_R$  is the electric double-layer interaction free energy per unit area between two flat parallel plates.

For simplicity we have ignored the effect of retardation<sup>11</sup> on the van der Waals force, so

$$V_A = -A_H/12\pi H^2$$

<sup>†</sup> This work was presented at the 8th International conference on Surface and Colloid Science, Adelaide, 13–18th Feb 1994.

<sup>‡</sup> University of Melbourne.

<sup>§</sup> CSIRO Division of Chemicals and Polymers.

\* Authors to whom correspondence should be addressed.

<sup>⊗</sup> Abstract published in *Advance ACS Abstracts*, January 1, 1995.

where  $A_H$  is the Hamaker constant<sup>12</sup> and  $H$  is the distance of closest approach between the sphere and the plate or between the two spheres. The Hamaker constant for the silica–titania system was calculated using the method of Hough and White<sup>13</sup> within the framework of Lifshitz theory.<sup>14</sup> A value of  $1.4 \times 10^{-20}$  J was obtained.

The electrical double-layer interaction,  $V_R$ , has been calculated for the constant-potential or constant-charge limits of the nonlinearized Poisson–Boltzmann equation using the method of McCormack et al.<sup>8</sup> For comparison the low-potential approximation of Hogg et al.<sup>7</sup> has also been used to calculate  $V_R$  when measurements were made between two spheres.

## Experimental Section

**SiO<sub>2</sub> Colloids.** The sample of SiO<sub>2</sub> colloids (XPS analysis showed that their composition was that of glass) was a gift from Sylvia Underwood, ICI Australia. The colloids were mostly in the size range 5–20  $\mu\text{m}$  diameter. A single colloid was glued to the end of an AFM cantilever spring with a heat softening wax using the method previously described.<sup>2,3</sup> This assembly will be hereafter referred to as a colloid probe. The radius of the colloid probe was determined by either optical or scanning electron microscopy. The colloid probes were rinsed with ethanol and blown dry with nitrogen before use.

To enable measurements to be taken between a colloid probe and another silica colloid, dry colloidal silica powder was carefully sprinkled onto a hot flat metal plate covered with a very thin layer of the same wax used to glue the colloid to the spring cantilever. The wax was allowed to harden and any spheres not properly fixed to the plate were blown off with a strong jet of nitrogen.

**TiO<sub>2</sub> Crystal.** The rutile TiO<sub>2</sub> single crystal was the same crystal used in a previous AFM study.<sup>3</sup> It was obtained from Tioxide U.K. The crystal had been polished to optical smoothness and AFM images showed the RMS roughness to be approximately 3 nm over 10  $\mu\text{m}^2$ . The crystal was steamed cleaned with Milli-Q water for 5 h before use to remove any surface contamination. Electron spectroscopy for surface analysis (ESCA) indicated that there was less than 1% tin or lead present. X-ray diffraction results showed the crystal was rutile in structure. As with the colloid probes, the crystal was rinsed with ethanol and blown dry immediately before use.

**Reagents.** Analytical grade KNO<sub>3</sub>, KOH, and HNO<sub>3</sub> were used without further purification. High-grade nitrogen (99%) and AJAX AR grade ethanol were used as supplied. Millipore Milli-Q water was used throughout.

**Force Measurements.** The force measurements were taken with a Digital Instruments, Inc. (Santa Barbara, CA) Nanoscope III atomic force microscope. The technique used to make these measurements is well documented.<sup>2–4</sup> The AFM software generates a file containing the deflection of the cantilever versus the displacement of the flat surface toward and away from the cantilever. These data can readily be converted to force versus separation.<sup>2,3</sup> The spring constant of the cantilevers used in these experiments were determined by the method of Cleveland et al.<sup>15</sup> and were found to be  $0.1 \pm 0.01$  N/m. When identical cantilevers are used, this method has been shown<sup>16</sup> to give the same result as the method of Senden and Ducker.<sup>17,18</sup> The latter method of determining spring constants was employed in our earlier AFM study of titania interactions.<sup>3</sup>

When measurements were made between a colloid probe and another silica colloid, the polished stainless steel plate onto which a number of colloids had been glued was imaged with the AFM to find a suitable single isolated sphere. It should be mentioned that the reason a number of spheres were mounted

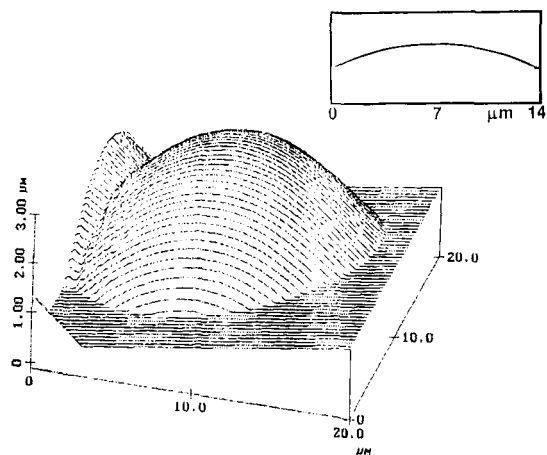


**Figure 1.** AFM image of silica colloid glued onto a polished metal plate. Only the top portion of the sphere can be seen because of the presence of nearby spheres and/or the partial embedment of the sphere in the wax matrix. The inset shows a section cut through this image, this section in combination with those from other directions to allow the average radius of the sphere to be calculated.

on to a plate was simply to help in locating a sphere in the  $XY$  range available for the scanner head used in the AFM. Imaging the sphere was necessary for two main reasons. First, the radius of the sample sphere needs to be measured as this is required to properly scale the force of interaction. Second, by imaging the sample sphere, it was possible to locate the apex of the sphere so that the two interacting spheres could be aligned through their centers in the direction of the interaction. Normally only the top portion of the sphere could be imaged because of the presence of nearby colloids and/or partial embedment of the colloid in the wax matrix; see Figure 1. The AFM software enabled a cross section to be cut through these images (see inset Figure 1), and from these sections it was possible to calculate the radius of the imaged sphere or, more precisely, the local radius of curvature. As a colloid was used to image the sphere, the overall  $XY$  dimensions were exaggerated and could not be used to determine the radius of the sphere; to lessen the effect of this distortion the largest sphere that could be found was chosen and only the data at the very apex of the image was used to calculate the radius of the sphere. To further minimize the error in fitting the radius, cross sections were taken both parallel and perpendicular to the direction of the scan on a number of images which were also taken at different scan angles.

## Results and Discussion

In Figure 2 we show examples of the force, scaled by the radius of the colloid probe, versus separation curves for the silica–titania system as the pH was varied between 8.8 and 3.3. The background electrolyte level was  $1.0 \times 10^{-3}$  M KNO<sub>3</sub>. The initial strong, long-range electrostatic repulsion is seen to decrease as the pH is decreased and turns to an attraction at pH 5.1. This trend is in qualitative accord with the expected behaviour based on what is known about the variations of net charges on the surfaces of the two oxides as the pH decreases. The iep of the rutile titania single crystal is around pH 5.6,<sup>3</sup> whereas the iep of silica is around pH 3.<sup>19–21</sup> Therefore, below pH 5.6 there is an electrostatic attraction between the positively charged titania and the negatively charged silica. For pH above the iep of the titania crystal there is an electrostatic repulsion between the unequally charged negative surfaces.

In AFM force measurements between silica–silica<sup>2,4</sup> and titania–titania,<sup>3</sup> the electrical double-layer interaction is better

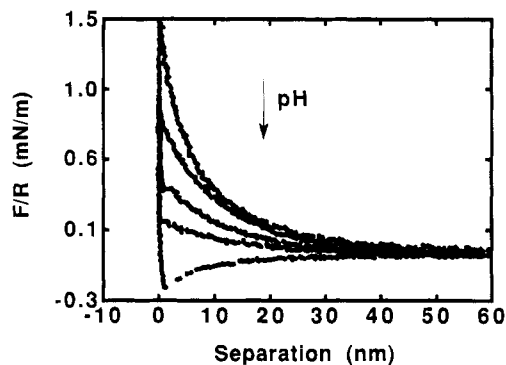


**Figure 2.** Examples of force, scaled by the radius of the colloid probe, versus separation curves for the silica-titania system. The curves correspond to pH values, from top to bottom, of 8.8, 7.2, 6.3, 5.3, and 3.0. The iep of silica is around pH 3, while the iep of titania is around pH 5.6. The degree of electrostatic repulsion decreases as the pH decreases, and at pH 3.0, i.e., below the iep of titania, there is an electrostatic attraction as well as the van der Waals attraction resulting in an overall attraction between the two surfaces.

modeled by the constant-charge boundary condition than the constant-potential condition. Solutions of the Poisson-Boltzmann equation predict, for constant-potential interactions between dissimilar surfaces of like sign, charge reversal of the less-charged surface can occur, and therefore the electrostatic interaction between the two surfaces at small separations becomes attractive.<sup>8,9</sup> Our experimental results show no evidence of this electrostatic attraction above the iep of titania which is consistent with our near-constant charge fits to the data.

For inorganic surfaces an extra non-DLVO repulsion at short range is sometimes observed. This additional short range force has been seen before in force-separation curves between silica in both the AFM<sup>2,4</sup> and the surface force apparatus (SFA).<sup>22-24</sup> For silica surfaces this extra short-range repulsion has been called a "hydration force"<sup>22,23</sup> but may actually be due to surface located polysilicates and therefore the repulsion may be steric/entropic in origin.<sup>24,25</sup> The force-separation curves for the silica-titania system at high pH (Figure 2) suggest that there may be an extra non-DLVO short-range repulsion. However, surface roughness considerations become important in these AFM measurements where the range of the surface force is of the same order as the surface roughness. Contact between asperities may lead to an apparent short range repulsion which would mimic this "hydration force". However, when measurements were made between silica surfaces directly after (<5 min) the injection of pure water, there was no evidence of an extra short-range repulsion. At small separations there was a "jump-in" that could be attributed to van der Waals interaction. The "jump-in" disappeared after a change of the aqueous solution conditions to  $10^{-3}$  M  $\text{KNO}_3$ . We did not study this aspect of the work in detail, but time development of an extra short-range repulsion between silica surfaces has been reported elsewhere.<sup>23</sup>

In Figure 3 we show theoretical force-separation curves for different pairs of potentials that when multiplied together give the same number. For constant charge systems there is very little difference between the curves produced by the different pairs of potentials. At large separations where theory is fitted to the experimental data to determine the diffuse-layer potentials, there is little difference between the constant-potential systems. Clearly, there is not a unique pair of diffuse-layer potentials that fit the individual experimental force curves. Even when the constant-potential interaction fits are considered, any differences between different potential pairs at small separations may be obscured if there is an extra non-DLVO short-range

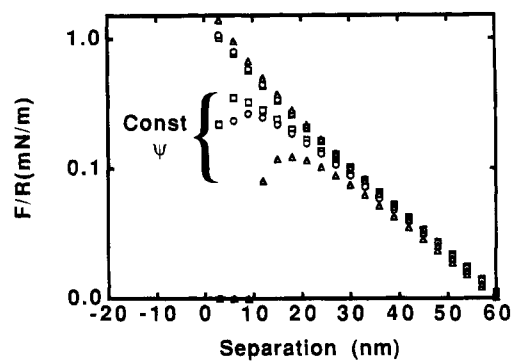


**Figure 3.** Theoretical force-separation curves for different pairs of potentials that when multiplied together give the same number. The symbols refer to the different potential pairs:  $\Delta$  -20 and -80 mV,  $\circ$  -53 and -30 mV,  $\square$  -40 and -40 mV. The upper three curves are the constant charge limits, while the lower three are the constant potential boundary conditions. There is very little difference between the three constant charge curves and at large separations there is very little difference between the constant potential curves. A Hamaker constant of  $1.4 \times 10^{-20}$  J was used in the calculations.

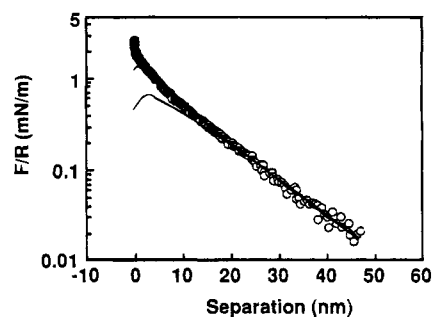


**Figure 4.** Force-separation curve taken between two silica spheres with radii of 8 and 21  $\mu\text{m}$  at pH 6.25 and a background electrolyte level of  $1 \times 10^{-3}$  M  $\text{KNO}_3$ . The upper fitted curve is the constant charge limit and the lower curve is the constant-potential limit. The fitting parameters are diffuse layer potential = -45 mV and Debye length = 9.6 nm. The extra non-DLVO short-range repulsion can clearly be seen. A Hamaker constant of  $0.8 \times 10^{-20}$  J was used in the calculations.<sup>13</sup>

repulsion. For this reason it was necessary to have independently obtained values of the diffuse layer potentials of the materials for comparison.

To obtain direct potential data for the silica colloids, force measurements were taken between two silica particles. In Figure 4 we show a force-separation curve taken between two silica spheres with radii of 8 and 21  $\mu\text{m}$  at pH 6.3 and a background electrolyte level of  $1.0 \times 10^{-3}$  M  $\text{KNO}_3$ . The experimental curve is fitted with both constant potential, lower solid curve, and constant charge, upper solid curve, solutions of the nonlinearized Poisson-Boltzmann equation with  $\Psi_d = -43$  mV and a Debye length of 9.6 nm. As can be seen, the interaction is closer to constant charge than constant potential. At small separations there is an apparent non-DLVO repulsion, as seen in the dissimilar surface interactions. By fitting the experimental force-separation curves with theory in this manner it is possible to obtain the diffuse layer potentials over a range of pH. The potentials obtained with an electrolyte level of  $1.0 \times 10^{-3}$  M  $\text{KNO}_3$  are shown in Figure 5. The pH, initially 6.3, was increased to pH 9.2 and then decreased incrementally. Below pH 5.1 the error in fitting potentials becomes large because of the apparent extra short-range repulsion added onto the small electrostatic repulsion, and for this reason potentials are not shown for pH less than 5.1. An extrapolation of the data to zero potential, shown as a dashed line in Figure 5, gives an iep of pH 2.5 which is similar to that obtained by other

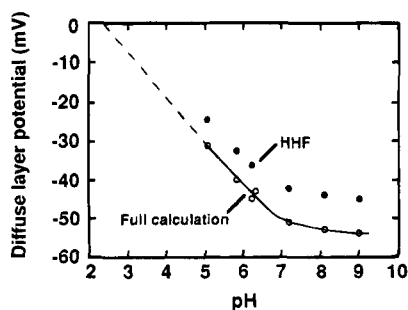


**Figure 5.** Diffuse-layer potentials obtained by the fitting procedure in Figure 4 as a function of pH at a background electrolyte level of  $1 \times 10^{-3}$  M  $\text{KNO}_3$ . The open circles refer to the potentials obtained using the full nonlinearized Poisson–Boltzmann equation. Below pH 5.1 the error in fitting the potentials became large because of the extra apparent short-range repulsion added onto the small electrostatic repulsion, and for this reason potentials are not shown for pH less than 5.1. The filled circles refer to the potentials obtained using the low potential approximation of Hogg et al.<sup>7</sup>

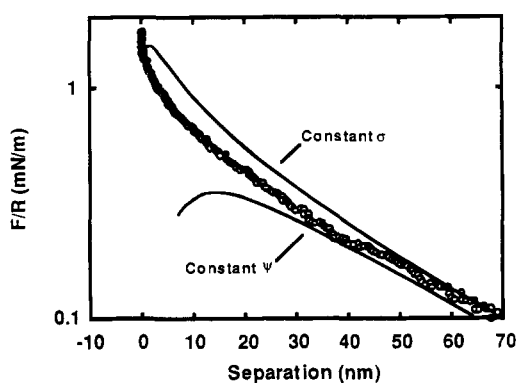


**Figure 6.** Force–separation curve for the silica–titania system taken at pH 8.8 and a background electrolyte level of  $1 \times 10^{-3}$  M  $\text{KNO}_3$ . The solid curves are theoretical curves using fitting parameters of diffuse layer potentials =  $-47$  and  $-38$  mV and Debye length =  $14$  nm. A Hamaker constant of  $1.4 \times 10^{-20}$  J was used in the calculations.

methods.<sup>19–21</sup> If the low-potential approximation of Hogg, Healy, and Fuerstenau (HHF)<sup>7</sup> is used the diffuse layer potentials obtained are 10–15% lower, as expected,<sup>7</sup> than those obtained using the full solution; see Figure 5. This is as expected considering the relatively large potentials obtained at high pH which put such systems outside the approximations used in the HHF method.

Microelectrophoretic mobility measurements have previously been made on a sample of titania<sup>3</sup> and were converted to  $\zeta$ -potentials using the Helmholtz–Smoluchowski equation.<sup>26</sup> These  $\zeta$ -potentials allow a comparison of potentials to be made with the information from the dissimilar surfaces AFM measurements.

The diffuse layer potentials from independent measurements were used as guides in fitting the dissimilar surfaces force–separation curves with theory. In Figure 6 we show a dissimilar surfaces force–separation curve taken at pH 8.8 with a salt concentration of  $1.0 \times 10^{-3}$  M  $\text{KNO}_3$ , it is fitted with diffuse layer potentials of  $-47$  mV for silica and  $-38$  mV for titania with a Debye length of  $14$  nm. This pH is above the titania's iep, and the force–separation curve shows an electrostatic repulsion and also an apparent extra short-range repulsion. Even though it is impossible to see a “jump-in” because of this apparent extra repulsion, the interaction is closer to constant charge than constant potential. A force–separation curve taken at a pH below the iep of the titania crystal shows an electrostatic attraction; see Figure 7. This curve, taken at pH 3.0, has been fitted with a silica potential of  $-5$  mV, a titania potential of

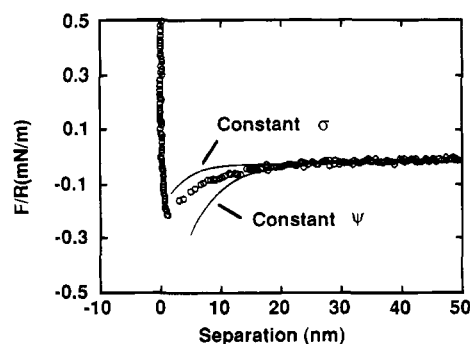


**Figure 7.** Force–separation curve for the silica–titania system taken at pH 3.0 and a background electrolyte level of  $1 \times 10^{-3}$  M  $\text{KNO}_3$ . The solid theoretical curves are based on fitting parameters of diffuse layer potentials =  $-5$  and  $+25$  mV and Debye length =  $9.6$  nm. A Hamaker constant of  $1.4 \times 10^{-20}$  J was used in the calculations. Note: this is a linear ( $F/R$ ) plot.

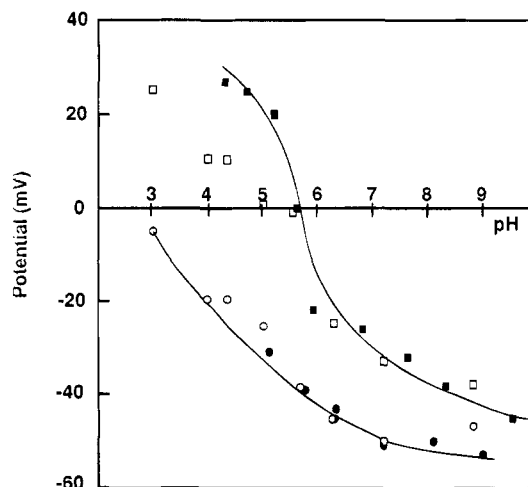


**Figure 8.** Comparison of the microelectrophoresis  $\zeta$ -potentials,  $\blacksquare$ , and the AFM diffuse layer potentials,  $\square$ , measured in the dissimilar surfaces system for titania as a function of pH at a background electrolyte level of  $1 \times 10^{-3}$  M  $\text{KNO}_3$ . There is good agreement between the two sets of data above the iep of titania but poor agreement below. Also shown is a comparison of the AFM silica sphere–sphere potential data,  $\circ$ , and the AFM silica dissimilar surfaces data,  $\bullet$ , as a function of pH at the same electrolyte level as the titania data.

$+25$  mV and a Debye length of  $9.6$  nm. Unlike force–separation curves showing electrostatic repulsion, attractive curves can be uniquely fitted with a positive and a negative potential. Independent information is still needed, however, in order to determine unambiguously which surface is positive and which is negative. The assignments of the sign of the potentials is entirely consistent with all other electrokinetic studies of these materials.

A comparison of the  $\zeta$  potentials and the diffuse-layer potentials measured in the dissimilar system for titania is shown in Figure 8. Both measurements were taken with a salt concentration of  $1.0 \times 10^{-3}$  M  $\text{KNO}_3$ . There is good agreement above the iep, pH 5.6, of the titania but below this pH agreement is poor. The dissimilar surfaces data indicates an iep for the rutile crystal at pH  $5.2 \pm 0.2$ , this is slightly lower than for the titania colloid but within experimental error of the microelectrophoresis result. Also, the crystal does not seem to charge as highly on the positive side as the colloid sample. A likely reason for this poor correspondence is that it is difficult to accurately obtain  $\Psi_d$  values for low-magnitude force–separation curves (see Figure 7), as already indicated for the  $\text{SiO}_2$  data.

A comparison of the silica sphere–sphere potential data with the silica dissimilar surfaces data is also shown in Figure 8.

There is good agreement between the potentials measured with the two methods.

### Conclusions

Collectively, it can be concluded that DLVO theory can adequately describe the interaction of the dissimilar titania and silica surfaces at large to near-contact separations. At separations of less than 2 nm, repulsive forces in excess of DLVO forces may be present under certain circumstances, i.e., the presence of electrolyte and a moderately to highly charged silica surface. Modeling of the force–separation curves is best described by a constant-charge condition rather than constant-potential boundary condition for both the identical system and the dissimilar system (where one can have different surface potentials of the same or opposite sign in isolation). The experimental data are seen to fall between constant potential and constant charge, though closer to constant charge. A more accurate fit of the experimental data may require charge regulation models for SiO<sub>2</sub> and TiO<sub>2</sub> which would bring in additional parameters.

**Acknowledgment.** I.L. acknowledges the support of an Australian Postgraduate Research Award. This work was supported by a grant from the Australian Research Council (ARC). Support from the ARC Advanced Minerals Products Special Research Centre and the ICI U.K. Strategic Research Fund is also gratefully acknowledged. The authors thank Dr. R. Hayes for determining the composition of the SiO<sub>2</sub> colloids.

### References and Notes

- (1) Binnig, G.; Quate, C.; Gerber, G. *Phys. Rev. Lett.* **1986**, *56*, 930.
- (2) Ducker, W. A.; Senden, T. J.; Pashley, R. M. *Langmuir* **1992**, *8*, 1831.
- (3) Larson, I.; Drummond, C. D.; Chan, D. Y. C.; Grieser, F. *J. Am. Chem. Soc.* **1993**, *115*, 11885.
- (4) (a) Ducker, W. A.; Senden, T. J.; Pashley, R. M. *Nature* **1991**, *353*, 239. (b) Butt, H.-J. *Biophys. J.* **1991**, *60*, 1438. (c) Meagher, L. *J. Colloid Interface Sci.* **1992**, *152*, 293.
- (5) (a) Rutland, M. W.; Senden, T. J. *Langmuir* **1993**, *9*, 412. (b) Li, Y. Q.; Tao, N. J.; Pan, J.; Garcia, A. A.; Lindsay, S. M. *Langmuir* **1993**, *9*, 637. (c) Karaman, M. E.; Meagher, L.; Pashley, R. M. *Langmuir* **1993**, *9*, 1220. (d) O'Shea, S. J.; Welland, M. E.; Rayment, T. *Langmuir* **1993**, *9*, 1826. (e) Atkins, D. T.; Pashley, R. M. *Langmuir* **1993**, *9*, 2232. (f) Biggs,

S. R.; Milling, A. J. *J. Colloid Interface Sci.*, in press. (g) Senden, T. J.; Drummond, C. J.; Kekicheff, P. *Langmuir* **1994**, *10*, 358. (h) Biggs, S. R.; Mulvaney, P. *J. Chem. Phys.* **1994**, *100*, 8501. (i) Rabinovich, Ya.I.; Yoon, R.-H. *Langmuir* **1994**, *10*, 1903. (j) Drummond, C. J.; Senden, T. J. *Colloids Surf.* **1994**, *87*, 217. (k) Senden, T. J.; Drummond, C. J. *Colloids Surf.*, in press.

- (6) Derjaguin, B. V.; Landau, L. *Acta Physicochem.* **1941**, *14*, 633.
- Verwey, E. G. W.; Overbeek, J. T. G. *The Theory of the Stability of Lyophobic Colloids*; Elsevier: Amsterdam, 1948.
- (7) Hogg, R.; Healy, T. W.; Fuerstenau, D. W. *Trans. Faraday Soc.* **1966**, *62*, 1638.
- (8) McCormack, D.; Carnie, S. L.; Chan, D. Y. C. *J. Colloid Interface Sci.*, in press.
- (9) Chan, D. Y. C.; Healy, T. W.; White, L. R. *J. Chem. Soc., Faraday Trans 1* **1976**, *72*, 2845.
- (10) Derjaguin, B. V. *Kolloid-Z.* **1934**, *69*, 155.
- (11) Most colloid and surface science texts will present a section on this. A very good account is given by: Hunter, R. J. *Foundations of Colloid Science*, Oxford, 1989; Vol. I, p 188.
- (12) Hamaker, H. C. *Physics* **1937**, *4*, 1058.
- (13) Hough, D. B.; White, L. R. *Adv. Colloid Interface Sci.* **1980**, *14*, 3.
- (14) Lifshitz, E. M. *Sov. Phys. JETP* **1956**, *2*, 73.
- (15) Cleveland, J. P.; Manne, S.; Bocek, D.; Hansma, P. K. *Rev. Sci. Instrum.* **1993**, *64*, 403.
- (16) Drummond, C. J.; Larson, I.; Mulvaney, P. C., unpublished results.
- (17) Senden, T. J.; Ducker, W. *Langmuir* **1994**, *10*, 1003.
- (18) Drummond, C. J.; Senden, T. J. Characterisation of the Mechanical Properties of Thin Film Cantilevers with the Atomic Force Microscope. Proceedings of INTERFACES II, Materials Science Forum, Trans Tech Publications Ltd.: Aedermansdorf, Switzerland, in press.
- (19) Parks, G. A. *Chem. Rev.* **1965**, *65*, 177.
- (20) Healy, T. W.; James, R. O.; Cooper, R. The Adsorption of Aqueous Co(II) at the Silica–Water Interface. In *Adsorption from Aqueous Solution*; *Adv. Chem. Ser.* **1968**, *79*, 62.
- (21) Grieser, F.; Lamb, R. N.; Wiese, G. R.; Yates, D. E.; Cooper, R.; Healy, T. W. *Radiat. Phys. Chem.* **1984**, *23*, 43.
- (22) (a) Horn, R. G.; Smith, D. T.; Haller, W. *Chem. Phys. Lett.* **1989**, *162*, 404. (b) Horn, R. G.; Smith, D. T. *J. Non-Cryst. Solids* **1990**, *120*, 72. (c) Grabbe, A.; Horn, R. G. *J. Colloid Interface Sci.* **1993**, *157*, 375. (d) Parker, J. L.; Yaminsky, V. V.; Claesson, P. M. *J. Phys. Chem.* **1993**, *97*, 7706. (e) Parker, J. L.; Rutland, M. W. *Langmuir* **1993**, *9*, 1965.
- (23) Chapel, J.-P. *J. Colloid Interface Sci.* **1994**, *162*, 517.
- (24) Vigil, G.; Xu, Z.; Steinberg, S.; Israelachvili, J. N. *J. Colloid Interface Sci.* **1994**, *165*, 367.
- (25) Healy, T. W. In *The Colloid Chemistry of Silica*; Bergna, H. E., Ed. *Adv. Chem. Ser.* **234**; American Chemical Society: Washington DC, 1994; Chapter 7.
- (26) Hiemenz, P. C. *Principles of Colloid and Surface Chemistry*, 2nd ed.; Dekker: New York, 1986; p 751.

JP942364H